SFERA-III

Solar Facilities for the European Research Area

Accuracy of Transient Linear Fresnel Collector Testing

Deliverable D10.4 / D39

Estimated delivery date:	31.12.2021
Actual delivery date:	20.01.2022
Lead beneficiary:	Fraunhofer ISE
Person responsible:	Schöttl, Peter
Deliverable type:	☒ R ☐ DEM ☐ DEC ☐ OTHER ☐ ETHICS ☐ ORDP
Dissemination level:	☒ PU ☐ CO ☐ EU-RES ☐ EU-CON ☐ EU-SEC

THIS PROJECT HAS RECEIVED FUNDING FROM THE EUROPEAN UNION'S HORIZON 2020 RESEARCH AND INNOVATION PROGRAMME UNDER GRANT AGREEMENT NO **823802**

AUTHORS

Author	Institution	E-mail
Peter Schöttl	Fraunhofer ISE	peter.schoettl@ise.fraunhofer.de
Alaric Montenon	Cyprus Institute	a.montenon@cyi.ac.cy
Costas Papanicolas	Cyprus Institute	cnp.energy@cyi.ac.cy
Stephen Perry	Fraunhofer ISE (formerly)	perry.metric@gmail.com
Anna Heimsath	Fraunhofer ISE	anna.heimsath@ise.fraunhofer.de

DOCUMENT HISTORY

Version	Date	Change
1.0	11.01.2022	First version
1.1	17.01.2022	Corrected formatting
1.2	20.01.2022	Minor modifications

VALIDATION

Reviewers		Validation date
Marc Röger	DLR	11.01.2022

DISTRIBUTION LIST

Date	Recipients
20.01.2022	Consortium

Disclaimer

Executive Summary

Modelling of the Linear Fresnel collectors in a real environment using standardized, state-of-the-art approaches is still inaccurate, yet it is crucial for robust loop control and collector yield assessment. Two advanced parameter identification methodologies – ParaID by Fraunhofer ISE and RealTrackEff by the Cyprus Institute – are compared in terms of the underlying equations, which extend ISO 9806. Both approaches are then applied to a Linear Fresnel collector research facility at the Cyprus Institute, for which a database of more than 50 measurement days is available, including reflectometric measurements. For both methods, several variations with increasing complexity are tested and the quality of the resulting fit in terms of outlet temperature is studied. Both methods take into account soiling/cleanliness and non-linear collector behaviour. While ParaID focuses on the identification of the IAMs in a real environment, the method by the Cyprus Institute links the efficiency to non-linear tracking effects. Real collector characteristics like varying cleanliness and asymmetric collector behaviour are found to have a strong impact on the collector performance and the identified parameters. For the ParaID approach, additional results regarding confidence intervals based on Bootstrapping and regarding identified Incidence Angle Modifiers are presented.

1. Introduction

The following text has been submitted as a conference paper: “Schöttl, Montenon, Papanicolas, Perry, Heimsath; *Comparison of Advanced Parameter Identification Methods for Linear Fresnel Collectors in Application to Measurement Data*; presented at SolarPACES2020 online conference; expected to be published in 2022”. The full publication covers the scope of this deliverable. The conference article is expected to be published in AIP proceedings in 2022.

Accurate parametric models for Linear Fresnel collectors (LFC) – obtained from testing data – are crucial, to allow for reliable performance predictions in operation on one hand, but also to allow for valid comparisons between different collector designs and technologies on the other hand (e.g. with yield assessment for certification). The existing ISO 9806 [1] standard is severely limited with regard to accurate assessment of LFCs. Therefore, several extended parameter identification methodologies have been developed to overcome these restraints. In this study, two methodologies – by Fraunhofer ISE and by the Cyprus Institute respectively – are introduced and then quantitatively compared to the original ISO 9806 and to each other, with respect to their ability in accurately depicting thermal measurements of an LFC installation at the Cyprus Institute.

2. Collector and Measurement data

The collector for the study has been in operation at the Cyprus Institute since July 2016, with the purpose of supplying heating and cooling to an adjacent building, the *Novel Technologies Laboratory* (Fig. 1 left) [2].

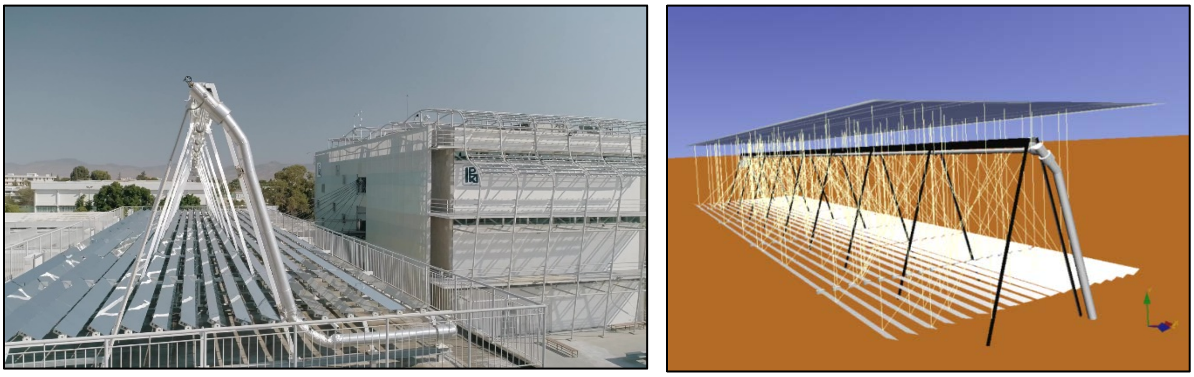

FIGURE 1. Left: Linear Fresnel collector and *Novel Technologies Laboratory* at the Cyprus Institute; right: rendering of the LFC ray tracing model in *Tonatiuh*

The LFC is made of 288 mirrors for the primary reflector with a net area A_{ap} of 184.32 m^2 and a collector length L_{coll} of 32 m. With Duratherm 450 as a heat transfer fluid (HTF), heat is exchanged with the storage loop of pressurized water. The maximum operational temperature is 180°C. The absorber is insulated with vacuum inside a borosilicate glass pipe. The present work relies on a campaign of 54 measurement days distributed between May 2018 and September 2019.

Both parameter identification methods rely on the following measured quantities:

- the absorber inlet and outlet temperatures T_{in} and T_{out}, sampled every 15s or 30s (with PT100, class 1/3 sensor from *TC Misuri e controlli*),
- the volumetric flow sampled every 15s or 30s, with a vortex flowmeter (*Proline Prowirl F 200*),
- the DNI with a pyrheliometer sampled each 1s (*LP Pyhre 16 AC* with *EKO STR 21G* tracker),
- the daily average specular reflectometry on 32 points of the primary reflector at

660nm (*Devices & Services 15R-USB* portable reflectometer),

- the ambient temperature T_{amb} with a weather station (*Davis Vantage Pro 2*).

The Cyprus Institute led research on the reflectometry techniques in order to determine the minimum number of measurements on a field required to estimate the level of error in reflectometry below 2.5% with 95% of confidence [3]. Consequently, soiling has been measured almost daily on 32 points of the primary reflector. However, the reflectometry only takes into account soiling on the primary optics; dust on the secondary reflector and on the borosilicate glass is not considered. The data sets have been either interpolated or averaged for the measurement time steps.

Furthermore, the following non-measured quantities have been used:

- the specific heat capacity c_p of the HTF, as given by the manufacturer as a function of temperature,
- the density ρ of the HTF, as given by the manufacturer as a function of temperature,
- the Incidence Angle Modifier (IAM) for each θ_t and θ_l, as obtained from ray tracing (see Fig. 1 right) with *Tonatiuh* [4].

3. Parameter Identification methods

As a basis for this study, two methodologies have been used that allow identifying the optical and thermal collector behaviour: *ParaID* by Fraunhofer ISE and *RealTrackEff* by the Cyprus Institute. Both methodologies determine coefficients of a collector equation modified from ISO 9806 [1]. A direct comparison of equation (1) applied by *ParaID* and equation (2) applied by *RealTrackEff* is given in the following:

$$\frac{\dot{Q}_{th}}{A_{ap}} = \eta_0 \cdot \xi_{clean}(t) \cdot \rho_{track}(\theta_t, \theta_l) \cdot IAM(\theta_t, \theta_l) \cdot DNI - c_1 \cdot (T_m - T_{amb}) - c_2 \cdot (T_m - T_{amb})^2 \quad - c_5 \cdot \frac{dT_m}{dt} \qquad (1)$$

$$\frac{\dot{Q}_{th}}{A_{ap}} = \eta_0 \cdot \xi_{clean}(t) \cdot \quad IAM(\theta_t, \theta_l) \cdot \quad DNI - c_1 \cdot (T_m - T_{amb}) - c_2 \cdot (T_m - T_{amb})^2 \quad \text{(in sim. model)} \qquad (2)$$

with measured (green) quantities:

- thermal output power $\dot{Q}_{th} = \dot{m} \cdot \int_{T_{in}}^{T_{out}} c_p(\tau) \cdot d\tau$
- the cleanliness ξ_{clean} defined as the ratio between the average reflectance and clean reflectance (92.4%)
- mean collector temperature $T_m = (T_{out} + T_{in})/2$
- calculated transversal and longitudinal solar incidence angles, θ_t and θ_l

and with identified (orange) terms:

- the nominal optical efficiency η_0
- the heat loss coefficients c_1, c_2
- the thermal inertia coefficient c_5 as identified in *RealTrackEff*. *ParaID* covers the thermal inertia of the collector with a physical model within the simulation.
- the tracking modified efficiency $\rho_{track}(\theta_t, \theta_l)$ as calculated in *RealTrackEff*
- the Incidence Angle Modifier $IAM(\theta_t, \theta_l)$. For *RealTrackEff*, this comes from ray tracing. For *ParaID*, this is directly identified.

The specifics of both methodologies are separately covered in the following.

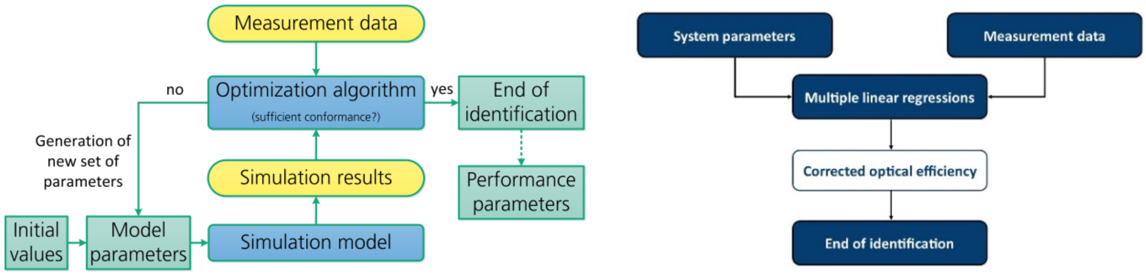

FIGURE 2. *ParaID* approach by Fraunhofer ISE (left). *RealTrackEff* methodology by Cyprus institute (right)

3.1. ParaID Approach by Fraunhofer ISE [5, 6]

In the *ParaID* approach, a set of solution values for the collector parameters to be identified is provided to an axially discretized, thermo-hydraulic collector model of the LFC, implemented in the Fraunhofer ISE software *ColSim CSP [7]*. From the simulation model, the transient collector behaviour is obtained for the measurement time periods. An optimizer compares simulation and measurement results and iteratively adjusts the identification parameters, until the best fit is found (see Fig. 2, left). Contrary to the classical ISO 9806 procedure, the underlying PlugFlow model [5] of the discretized absorber tube model represents the heat capacity of fluid and collector structures with real material models (instead of identifying c_5).

As a **base case**, η_0, c_1 and c_2 are identified with *ParaID*. A cleanliness $\xi_{clean} = 1$ is assumed, which implies that all soiling effects result in a reduced reflectance and eventually in a lower η_0. IAM profiles in transversal and longitudinal directions are taken from ray tracing.

In the second variation, a **variable cleanliness** ξ_{clean} based on reflectometry measurements is integrated. This implies that nominal reflectance (as part of *identified* η_0) and *measured* cleanliness are separated. An average cleanliness value for each measurement day is used, which is assumed to be a reasonable simplification, as long as there are no major weather events like thunderstorms or cleaning events within the day.

In the third variation, **IAM identification** is added, where the transversal and longitudinal IAM profiles are determined on a series of discrete, equidistant angle nodes, instead of obtaining them from ray tracing. IAM identification implies a large number of additional degrees of freedom, as compared to the base case. Thus, it is only possible if the database is sufficiently large (more than 12 measurement days [5]), which is the case in this study. Furthermore, IAM identification is only possible on angle nodes for which sufficient measurement data (usually in terms of cumulative DNI) is available. Thus, the resulting IAM curves are usually not covering the full angle range.

In the fourth variation, both **variable cleanliness ξ_{clean} and IAM identification** – as described in the second and third variation respectively – are combined. This represents the most sophisticated *ParaID* variation within this study and is expected to yield the most accurate results.

More detailed information on the *ParaID* approach is provided by Zirkel-Hofer et al. [5, 6], who originally authored and implemented the methodology.

3.2. RealTrackEff Approach by the Cyprus Institute [8]

RealTrackEff starts with the offline calculation of the $IAM(\theta_t, \theta_l)$ with Tonatiuh software for each transversal angle θ_t and each longitudinal angle θ_l with a step of 1° on each (91 x 91 values for the whole characterization), avoiding factorization. In the real environment, the optical performance strays from the ray-tracing environment due to several factors. On one hand, the soiling decreases radically the reflectivity of the mirrors, but also the transmissivity of the borosilicate glass that encloses the absorber. The estimation of such effect can be partially estimated with the reflectometry measurements on the primary reflector only and at 660 nm to determine ξ_{clean}. The manufacturing process of the mirrors and ageing modify the shape their idle conception. On the other hand, the real tracking operation is not continuous but position corrections are applied for each or couple of milliradians of error. Also, errors are due to mechanical frictions, slack, etc. on the gears. These elements are difficult to quantify for each of the transversal and longitudinal angles. This leads to spillage and therefore optical losses that are not quantified in the raytracing environment. Thus, in order to quantify them, the term $\rho_{track}(t)$ has been added to the model. The thermal power is exposed for two different days (May 3, 2018 and July 20, 2019, see Fig. 3 and Fig. 4). While DNI remains quite symmetric around the solar noon, the thermal power is not, and tends to decrease in the afternoon. This is only shown for two days here. The campaign of 54 days encloses more than 10^5 measurement times. This phenomenon could be observed in other days. This corresponds to a growing value in azimuth. So, Table 1 compares the 4 different methods applied by the Cyprus Institute to fit the measured temperature with the models proposed. First it is done by directly applying the ISO 9806 without taking into account the reflectometry ($\xi_{clean}(t) = 1$) nor the tracking corrections $\rho_{track}(t) = 1$. In a second step, the reflectivity is featured as part of the cleanliness, while the tracking errors are still considered to be $\rho_{track}(t) = 1$. In a third step, the linear influences of the longitudinal and transversal angles are added ($n = 1$). In the *RealTrackEff*, the last step, the degree is set to $n = 2$. Based on the above-mentioned parameters, the Cyprus Institute applies on them multi-linear regressions to proceed to the fitting (see Fig. 2, right).

TABLE 1. *RealTrackEff* methodology variations applied by the Cyprus Institute

RealTrackEff variation	**Optical efficiency**
ISO 9806	$\xi_{clean}(t) = 1$ $\rho_{track}(t) = 1$
ISO 9806 + reflectivity	$\xi_{clean}(t)$ based on the reflectometry measurements $\rho_{track}(t) = 1$
ISO 9806 + reflectivity + tracking error	$\xi_{clean}(t)$ based on the reflectometry measurements $\rho_{track}(t) = \sum_{k=0}^{n}\sum_{l=0}^{n}\left(\eta_{k,l} \cdot {\theta_t}^k \cdot {\theta_t}^l\right), n\epsilon[\![1,2]\!], 1 \leq l + k \leq 2$

4. Performance results and comparison of parameter identification methodologies

To characterize the performance of the investigated collector, the results for the nominal optical efficiency η_0 and for the length-specific heat losses are presented. The latter are chosen as they are easier to comprehend, as compared to the rather abstract coefficients c_1 and c_2. The length-specific heat losses $HL_{115°C}$ (W/m) are evaluated for a (typical) temperature difference $T_m - T_{amb} = 115°C$ to the ambient, with the following equation:

$$HL_{115°C} = c_1 \cdot \frac{A_{ap}}{L_{coll}} \cdot (T_m - T_{amb}) + c_2 \cdot \frac{A_{ap}}{L_{coll}} \cdot (T_m - T_{amb})^2 \tag{3}$$

Furthermore, in order to evaluate a set of identified parameters with regard to the resulting outlet temperature fit, the Root-Mean-Square of the temperature deviations is calculated as follows:

$$RMS_T = \sqrt{\frac{1}{n}\sum_{i=1}^{n}\left(T_{out,meas,i} - T_{out,sim,i}\right)^2} \tag{4}$$

where n is the number of measurement samples, $T_{out,meas,i}$ and $T_{out,sim,i}$ are the measured and simulated outlet temperatures of sample i respectively.

For the variations of the *ParaID* approach, results for all three quantities are presented in Table 2.

TABLE 2. Results from Fraunhofer ISE, ParaID

Method variation	$\boldsymbol{\eta_0}$[%]	$\boldsymbol{HL_{115°C}}$ [$\boldsymbol{W/m}$]	$\boldsymbol{RMS_T}$ [°$\boldsymbol{C}$]
Base case: η_0, c_1, c_2	32.7	192	2.24
+ Variable cleanliness ξ_{clean}	36.8	109	1.94
+ IAM identification	31.4	217	1.81
+ Variable cleanliness ξ_{clean}+ IAM identification	32.0	110	1.48

For the base case, a RMS_T of 2.24°C is obtained. Here, soiling effects are included in η_0, as no separate cleanliness factor is considered. By integrating variable cleanliness values < 1, a significant improvement of the temperature fit is achieved. Furthermore, η_0 increases, as a part of the optical losses is covered by the cleanliness factor. The lowest obtained RMS_T of 1.48°C is achieved by integrating both ξ_{clean} and IAM identification. The nominal optical efficiency is in turn reduced, which is due to significant differences between IAM profiles from ray tracing and from identification (see section on IAM profiles). For this latter case, RMS_T is higher than its equivalent for the *RealTrackEff* approach, which is attributed to the fact that the current implementation of IAM identification in *ParaID* doesn't allow for asymmetric IAM profiles. Yet, this seems to be characteristic for the collector under investigation.

For the variations of the *RealTrackEff* approach, results for all three quantities are presented in Table 3.

TABLE 3. Results from the Cyprus Institute, RealTrackEff

Method variation	$\boldsymbol{\eta_0}$[%]	$\boldsymbol{HL_{115°C}}$ [$\boldsymbol{W/m}$]	$\boldsymbol{RMS_T}$[°$\boldsymbol{C}$]
Base case: η_0, c_1, c_2	34.8	78	1.97
+ Variable cleanliness ξ_{clean}	29.2	97	1.59
+ Variable cleanliness ξ_{clean} + tracking efficiency (n=1)	29.2*	121	1.25
+ Variable cleanliness ξ_{clean} + tracking efficiency (n=2)	29.2*	31	0.99

* η_0 set to value from "Variable cleanliness ξ_{clean}" variation, as it is included in the tracking efficiency

RMS_T obtained in the base case for the Cyprus Institute is 1.97°C with a nominal optical efficiency value of 34.8%, disregarding the soiling effects. As the complexity of the model increases, the value decreases down to 0.99°C, taking the asymmetric behaviour into account, as described in Table 1.

For both methodologies, the most sophisticated variation with the most degrees of freedom achieves the lowest RMS_T. The resulting nominal optical efficiency η_0 values are close: 32% and 29.2% for *ParaID* and *RealTrackEff* respectively. For the length-specific heat losses $HL_{115°C}$, the differences are larger (see also section on Bootstrapping). As the heat losses are usually a small quantity that is dominated by the optical efficiency, their identification is less robust.

4.1. Exemplary Time Series and Temperature Fit Quality

For two exemplary measurement days (May 3, 2018 and July 20, 2019), the time series for measured and simulated outlet temperature are illustrated, along with other characteristic operation data.

Figure 3 presents the results for the *ParaID* methodology, in its most sophisticated variation (variable cleanliness ξ_{clean} and IAM identification).

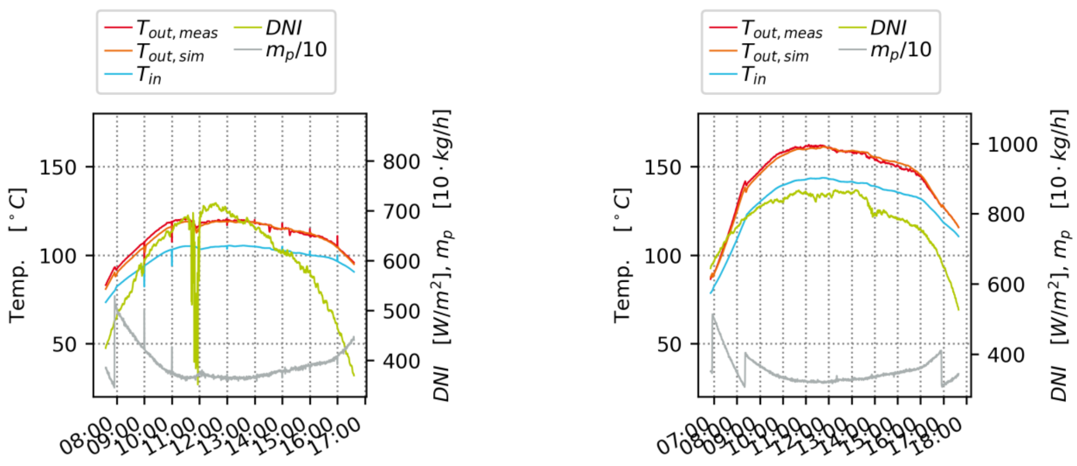

FIGURE 3. ParaID: time series for DNI, mass flow rate, inlet temperature and outlet temperature (measured/simulated), for May 3, 2018 (left) and July 20, 2019 (right)

For all operating conditions, the visualization shows a high conformance between simulation and measurement. Notably, the potential asymmetry of the collector manifests itself in the simulated collector outlet temperature that underestimates the measurements in the mornings and overestimates them in the afternoons.

Figure 4 presents the results for the *RealTrackEff* methodology, in its most sophisticated variation (variable cleanliness ξ_{clean} + tracking efficiency (n=2)).

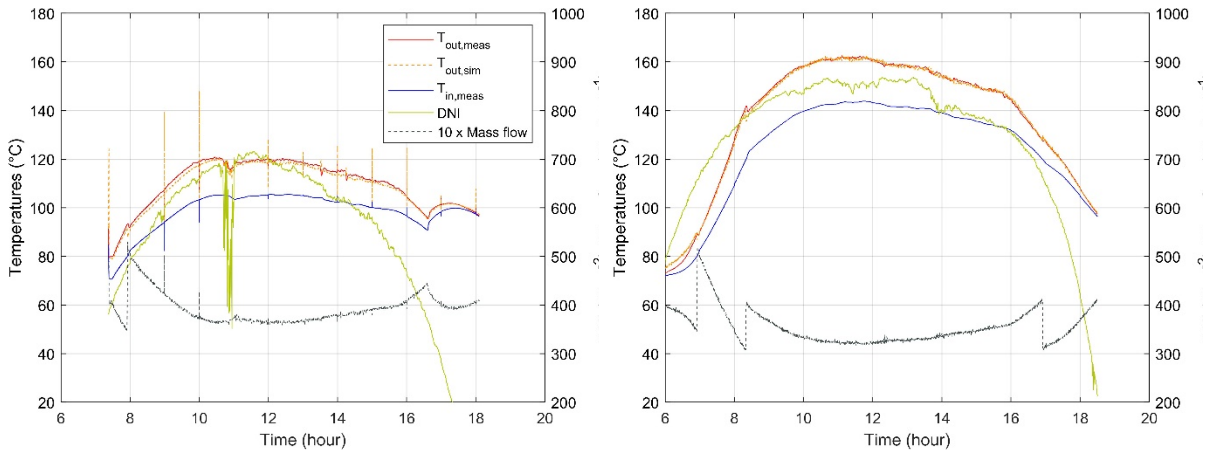

FIGURE 4. RealTrackEff: time series for DNI, mass flow rate, inlet temperature and outlet temperature (measured/simulated), for May 3, 2018 (left) and July 20, 2019 (right)

The methodology renders quite efficiently the asymmetric profile of the temperature output along the day, as it can be observed for both days, while DNI stays symmetric. This corrects the lack of asymmetry in the idealized IAMs from ray tracing. This empiric fitting reflects in a robust manner the nonlinear effects that are not considered in the ISO 9806. The inclusion of reflectometry takes into account the soiling on the primary reflector. However, dust deposits also affect the secondary optics and more importantly the borosilicate glass. So the cleanliness parameter only tackles an aspect of the soiling that can be corrected by the inclusion of the tracking efficiency as in *RealTrackEff*.

4.2. Confidence Interval Calculation for ParaID Approach with Bootstrapping

Figure 5 presents a confidence interval calculation based on a Bootstrapping approach [9] for the ParaID approach. Bootstrapping is a technique, where artificial data sets – obtained from resampling of the original measurement data – allow generating a probability distribution for the identification results. 95% confidence intervals are calculated for η_0 and $HL(115\,°C)$ identified with the method variation including variable cleanliness and IAM identification.

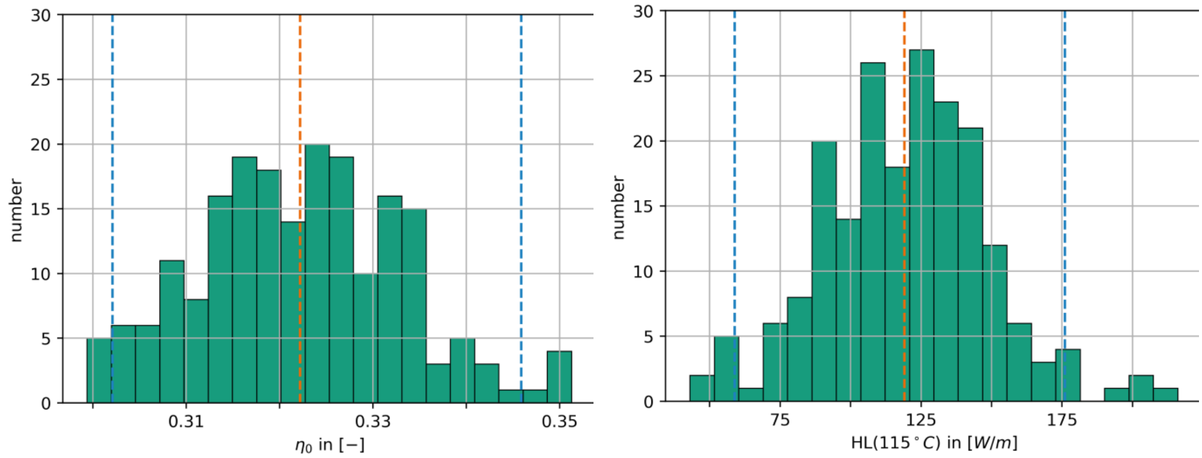

FIGURE 5. Bootstrapping results and confidence intervals for the ParaID approach. Histograms are plotted for the method variation including variable cleanliness and IAM identification, with the number of occurrences of different values of η_0 and $HL(115\,°C)$ in the left and right figure respectively. The dashed orange line gives the respective mean value, while the dashed blue lines represent the lower and upper limits of the 95% confidence interval.

With a size of about ±2%-pts around the mean value, the confidence interval for the nominal optical efficiency is rather narrow. With respect to the absolute identified value, the confidence interval for the heat loss at 115°C temperature difference is much larger. This indicates that η_0 can be identified with a much lower uncertainty, as compared to c_1, c_2 and $HL(115°C)$. This meets the expectations (also according to the findings by Zirkel-Hofer [5]), as the heat losses have a small impact on the collector yield, in particular because the system is operated at relatively low temperatures.

4.3. Comparison of IAM Profiles from Ray Tracing and ParaID Identification

Figure 6 presents a comparison of IAM profiles obtained from ray tracing and with the ParaID methodology.

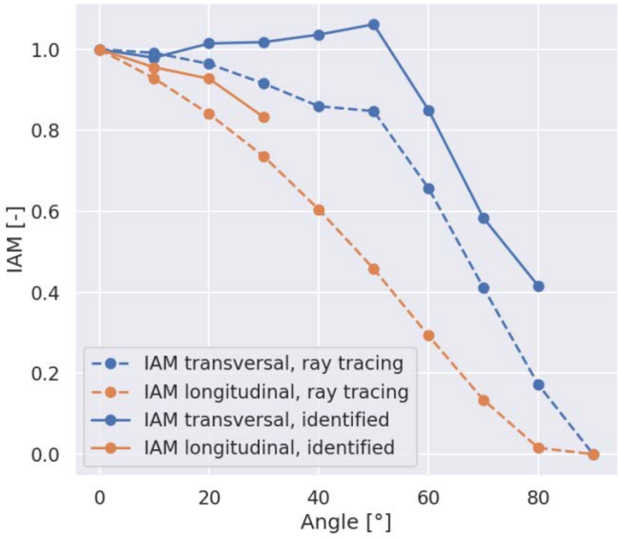

FIGURE 6. Comparison of transversal (blue) and longitudinal (orange) IAM profiles obtained from ray tracing (dashed lines) and with the ParaID methodology (solid lines). The latter can only be identified on the angle ranges for which sufficient measurement data is available.

The identified IAM profiles – where available – differ drastically from the ideal ray tracing results, for both the transversal and longitudinal directions. Reasons might include effects like tracking errors, collector misalignment, etc., which are not covered in an idealized ray tracing. For more clarity, further investigations are necessary. This finding agrees with the significantly higher identification quality of *ParaID* variations with activated IAM identification (see Table 2).

Generally, the importance of covering real optical collector behaviour (e.g. by IAM identification) is highlighted. Furthermore, asymmetric optical collector behaviour has been found, as pointed out in *RealTrackEff*. The integration of this aspect in the *ParaID* methodology will be part of future work.

5. Conclusion

Accurately identifying in-situ collector parameters and consequently deriving a model for a real facility is crucial for performance predictions during operation – allowing for robust control strategies – and in the certification process. This is particularly important for environments where strong deviations of the real collector behaviour from idealized representations occur.

Within this study, soiling/cleanliness and asymmetric collector behaviour have been identified as causes for such deviations and have been tackled. The presented methodologies by Fraunhofer ISE and the Cyprus Institute significantly improve the process of collector identification as compared to the state-of-the-art (ISO 9806).

6. Acknowledgments

The research that led to these results has received funding from the European Union's Horizon 2020 research and innovation programme under grant agreements No 823802 (SFERA-III) and No 731287 (INSHIP).

7. References

1.Solar energy - Solar thermal collectors - Test methods (DIN EN ISO 9806:2017), 9806:2017, 2017.

2.A. C. Montenon, N. Fylaktos, F. Montagnino, F. Paredes, and C. N. Papanicolas, “Concentrated solar power in the built environment,” in *SOLARPACES 2016*, Abu Dhabi, United Arab Emirates, 2017, p. 40006.

3.A. M. Bonanos, A. C. Montenon, and M. J. Blanco, “Estimation of mean field reflectance in CST applications,” *Sol Energy*, vol. 208, pp. 1031–1038, 2020.

4.J. P. Cardoso *et al.,* “New functionalities for the Tonatiuh ray-tracing software,” in *SOLARPACES 2017*, Santiago, Chile, 2018, p. 210010.

5.A. Zirkel-Hofer, “Enhanced dynamic performance testing method for line-concentrating solar thermal collectors,” Dissertation, Technische Universität Carolo-Wilhelmina zu Braunschweig, Braunschweig, 2018.

6.A. Zirkel-Hofer, K. Kramer, A. Heimsath, S. Scholl, and W. J. Platzer, “Dynamic performance evaluation of line-concentrating steam collectors,” in *AIP Conference Proceedings SolarPACES 2017*, Santiago, Chile, 2018, p. 30020.

7.C. Wittwer, “ColSim - Simulation von Regelungssystemen in aktiven solarthermischen Anlagen,” Universität Karlsruhe, Fakultät für Architektur, 1999.

8.A. C. Montenon, P. Tsekouras, C. Tzivanidis, M. Bibron, and C. Papanicolas, “Thermo-optical modelling of the linear Fresnel collector at the Cyprus institute,” *AIP Conference Proceedings*, vol. 2126, no. 1, p. 100004, 2019.

9.A. Zirkel-Hofer *et al.,* “Confidence interval computation method for dynamic performance evaluations of solar thermal collectors,” *Sol Energy*, vol. 162, pp. 585–596, 2018.